The Information Of The Milky Way From 2MASS Whole Sky Star Count: The Structure Parameters

Chan-Kao Chang[1]

Institute of Astronomy, National Central University, Jhongli, Taiwan

Chung-Ming Ko[2]

Institute of Astronomy, Department of Physics and Center of Complex Systems, National Central University, Jhongli, Taiwan

Department of Physics, University of Hong Kong, Pokfulam Road, Hong Kong

and

Ting-Hung Peng

Institute of Astronomy, National Central University, Jhongli, Taiwan

Received _____; accepted _____

[1]rex@astro.ncu.edu.tw

[2]cmko@astro.ncu.edu.tw

ABSTRACT

The K_s band differential star count of the Two Micron All Sky Survey (2MASS) is used to derive the global structure parameters of the smooth components of the Milky Way. To avoid complication introduced by other fine structures and significant extinction near and at the Galactic plane, we only consider Galactic latitude $|b| > 30^\circ$ data. The star count data is fitted with a three-component model: double exponential thin disk and thick disk, and a power law decay oblate halo. Using maximum likelihood the best-fit local density of the thin disk is $n_0 = 0.030 \pm 0.002$ stars/pc^3. The best-fit scale-height and length of the thin disk are $H_{z1} = 360 \pm 10$ pc and $H_{r1} = 3.7 \pm 1.0$ kpc, and those of the thick disk are $H_{z2} = 1020 \pm 30$ pc and $H_{r2} = 5.0 \pm 1.0$ kpc, the local thick-to-thin disk density ratio is $f_2 = 7 \pm 1\%$. The best-fit axis ratio, power law index and local density ratio of the oblate halo are $\kappa = 0.55 \pm 0.15$, $p = 2.6 \pm 0.6$ and $f_h = 0.20 \pm 0.10\%$, respectively. Moreover, we find some degeneracy among the key parameters (e.g., n_0, H_{z1}, f_2 and H_{z2}). Any pair of these parameters are anti-correlated to each other. The 2MASS data can be well-fitted by several possible combinations of these parameters. This is probably the reason that there is a wide range of values for the structure parameters in literature similar to this study. Since only medium and high Galactic latitude data are analyzed, the fitting is insensitive to the scale-lengths of the disks.

Subject headings: Galaxy: general - Galaxy: stellar content - Galaxy: structure - Galaxy: fundamental parameters - infrared: stars

1. Introduction

In the eighteenth century, the famous astronomer William Herschel showed us the powerful method of star count to understand our own Milky Way (Herschel 1785). The technique has been used since then by generations of astronomers. With great improvement on data collection over the years, more and more details of our Milky Way were unfolded. However, the characteristic scales of smooth Galactic structures (i.e., disks and halo) obtained by previous studies does not converge to a common value as an outcome of improving data collection (see Table 1). The spread of values is attributed to the degeneracy of Galactic model parameters (i.e., same star count data could be fitted equally well by different Galactic models) (Chen et al. 2001; Siegel et al. 2002; Jurić et al. 2008; Bilir et al. 2008). This is due to the different sky regions and limiting magnitudes (i.e., limiting volumes) used in these studies (Siegel et al. 2002; Karaali et al. 2004; Bilir et al. 2006a,b; Jurić et al. 2008). On the contrary, Bilir et al. (2008); Yaz & Karaali (2010) did not show such degeneracy in determining the Galactic model parameters. This controversy is still actively debated. Therefore, systematic all sky surveys with deeper limiting magnitude and wider sky region, such as the Two Micron All Sky Survey (2MASS; Skrutskie et al. 2006), the Sloan Digital Sky Survey (SDSS; York et al. 2000), the Panoramic Survey Telescope & Rapid Response System (Pan-Starrs; Kaiser et al. 2002) and the GAIA mission (Perryman et al. 2001) could provide a good opportunity for us to study our Galaxy from a global perspective. Free from limited sky fields, astronomers can acquire many more information from the stellar distribution of these surveys.

On Galactic structure study, besides the simple and smooth two-component model (Bahcall & Soneira 1980) or the three-component model (Gilmore & Wyse 1985), many more structures have been discovered, such as inner bars in the Galactic center (Alves 2000; Hammersley et al. 2000; van Loon et al. 2003; Nishiyama et al. 2005; Cabrera-Lavers et al.

2008), and flares and warps (Lopez-Corredoira et al. 2002; Robin et al. 2003; Momany et al. 2006; Reylé et al. 2009), which has been contributed the variation of disk model parameters with Galactic longitude (Cabrera-Lavers et al. 2007; Bilir et al. 2008; Yaz & Karaali 2010). Moreover, the overdensities in the halo, such as Sagittarius (Majewski et al. 2003), Triangulum-Andromeda (Rocha-Pinto et al. 2004; Majewski et al. 2004), Virgo (Jurić et al. 2008), and in the outer disk, such as Canis Major (Martin et al. 2004), Monoceros (Newberg et al. 2002; Rocha-Pinto et al. 2003), show the complexity of the Milky Way. The formation history of our Galaxy is more complicated than what we thought previously.

On stellar luminosity function study, a recent study by Chang et al. (2010) using the K_s band star count of 2MASS point source catalog (2MASS PSC; Cutri et al. 2003) verified for the first time the universality hypothesis of the luminosity function (i.e., the common practice of assuming one luminosity function for the entire Milky Way).

We are interested in the global smooth structure of our Galaxy. In view of the existing fine structures (e.g., flares, warps, overdensities...etc.), the structure of the smooth components can be determined either by including these fine structures in a grand Galaxy model or by avoiding the sky area "contaminated" with these features. The first method demands a complex model, which involves many more structure parameters, and needs high computing power to accomplish the fitting task. Lopez-Corredoira et al. (2002) is a good example of this method using 2MASS data. The second method is clearly simpler but needs justifications. We observe that (1) the fine structures (e.g., inner bars, flares and warps), which have observable contribution on 2MASS star count data, are all confined in the Galactic plane region. (2) The overdensities or substructures in the outer disk region and the halo are difficult to identify in general. Their contribution is negligible in the 2MASS star count data. Here we quote Majewski et al. (2004) on halo substructure: "This substructure is typically subtle and obscured by a substantial foreground veil of disk stars,

eliciting its presence requires strategies that optimize the substructure signal compared to the foreground noise."

We prefer the second method in this paper and only use Galactic latitude $|b| > 30°$ 2MASS K_s band star count data to obtain the structure parameters of a three-component model. In addition, the influence of the near infrared extinction in these regions is small. This also allows us to use a simpler extinction model for correction. We describe our model in section 2 and the analysis method in section 3. Section 4 provides the results and a discussion.

2. The Milky Way Model

We adopt a three-component model for the smooth stellar distribution of the Milky Way. It comprises a thin disk, a thick disk and an oblate halo (Bahcall & Soneira 1980; Gilmore & Reid 1983). The total stellar density $n(R, Z)$ at a location (R, Z) is the sum of the thin disk D_1, the think disk D_2 and the halo H,

$$n(R, Z) = n_0 \left[D_1(R, Z) + D_2(R, Z) + H(R, Z) \right] , \tag{1}$$

where R is the galactocentric distance on the Galactic plane, Z is the distance from the the Galactic mid-plane and n_0 is the local stellar density of the thin disk at the solar neighborhood.

The stellar distribution of the thin disk D_1 and the thick disk D_2 decreases exponentially along R and Z (the so called double exponential disk),

$$D_i(R, Z) = f_i \exp \left[- \frac{(R - R_\odot)}{H_{ri}} - \frac{(|Z| - |Z_\odot|)}{H_{zi}} \right] , \tag{2}$$

where $(R_\odot, Z_\odot)$ is the location of the Sun, H_{ri} is the scale-length, H_{zi} is the scale-height, and f_i is the density ratio to the thin disk at the solar neighborhood. The subscript $i = 1$

stands for the thin disk (thus $f_1 = 1$) and $i = 2$ for thick disk. We adopted $R_\odot = 8$ kpc in our model (Reid 1993).

The halo is a power law decay oblate spheroid flattening in the Z direction,

$$H(R, Z) = f_h \left[\frac{R^2 + (Z/\kappa)^2}{R_\odot^2 + (Z_\odot/\kappa)^2} \right]^{-p/2} , \tag{3}$$

where κ is the axis ratio, p is the power index and f_h is the local halo-to-thin disk density ratio.

Chang et al. (2010) showed that the whole sky K_s band luminosity function can be well approximated by a single power law with a power law index $\gamma = 1.85 \pm 0.035$, a bright cutoff at $M_b = -7.86 \pm 0.60$ and a faint cutoff at $M_f = 6.88 \pm 0.66$. We adopt this luminosity function in the following analysis. In normalized form, it is

$$\psi(M_{K_s}) = \frac{2 \log_e 10 \ (\gamma - 1)}{5 \left[10^{2(\gamma-1)M_f/5} - 10^{2(\gamma-1)M_b/5} \right]} \, 10^{2(\gamma-1)M/5} . \tag{4}$$

Note that $\psi(M)$ includes all luminosity classes. In our analysis the observing magnitude range is $5 \leq K_s \leq 14$ mag. The corresponding distances of bright cutoff, faint cutoff and $M_{K_s} = 0$ are 3.4 kpc to 216 kpc, 4 pc to 265 pc and 0.1 kpc to 6.3 kpc, respectively.

Although we only use NIR data in the medium and high Galactic latitude regions, we still need to correct possible interstellar extinction. We adopt the new COBE/IRAS result (Chen et al. 1999) and convert it to the K_s band extinction by $A_{K_s}/E(B-V) = 0.367$ (Schlegel et al. 1998). This extinction model is then applied to our simulation data. The extinction values of most of our analyzed regions are $A_{K_s} < 0.03$.

3. The Data and Analysis Method

3.1. The 2MASS Data

The 2MASS Point Source Catalog (2MASS PSC, Cutri et al. 2003) is employed to carry out the K_s band differential star count for the entire Milky Way. We divide the whole sky into 8192 nodes according to level 5 Hierarchical Triangular Mesh (HTM, Kunszt et al. 2001). The level 5 HTM samples the whole sky in roughly equal area with an average angular distance about 2 degrees between any two neighboring nodes. The amount of stars within 1 degree radius of each node (i.e., each node covers π square degree) is then retrieved with a bin size K_s=0.5 mag via 2MASS online data service (Cutri et al. 2003, catalog). Our selection criterion is: the object must be detected in all J, H, K_s bands and has signal-to-noise ratio ≥ 5. Since the limiting magnitude of 2MASS K_s band is 14.3 mag, which has 10 signal-to-noise ratio and 99% completeness (see Table 1 in Skrutskie et al. 2006), and $K_s \leq 5$ mag objects have relatively large photometric error, we only compare 2MASS data with our simulation data from $K_s = 5$ to 14 mag.

In order to minimize the effects coming from the close-to-Galactic-plane fine structures (e.g., flares, warps, arms, budge and bars...etc., which have considerable contribution to the star count data), and the relatively complex extinction correction at the low Galactic latitude region, we avoid low galactic latitudes, and only consider data in Galactic latitude $|b| > 30^\circ$. Although several overdensities in the halo (such as Sagittarius, Triangulum-Andromeda, Virgo...etc.) were identified, they cannot be picked up from the overwhelming foreground field stars on star count data without additional information (e.g., color, distance, metallicity...etc., Majewski et al. 2004). Therefore, their contribution to the 2MASS K_s band differential star count is negligible and will not affect our result. We also exclude the areas around Large and Small Magellanic Clouds for their significant stellar population.

3.2. The Analysis Method

The Maximum Likelihood Method (Bienayme et al. 1987) is applied to compare the K_s band 2MASS differential star counts and the simulation data to search for the best-fit structure parameters of the three-component Milky Way model. Our fitting strategy is as follows:

1. Take $R_\odot = 8$ kpc;
2. choose one $Z_\odot$ and work out the maximum likelihood value by fitting the 9 parameters $(n_0, H_{z1}, H_{r1}, f_2, H_{z2}, H_{r2}, f_h, \kappa, p)$;
3. repeat step 2 for other $Z_\odot$;
4. pick the $Z_\odot$ corresponds to the maximum of the maximum likelihood values in step 3;
5. repeat steps 2 to 4 for finer grid size of the 9-parameter fit and a narrower range of $Z_\odot$ around the one found in step 4;
6. the uncertainty is estimated by adding Poisson noise on the simulation data to see how the likelihood varies. The difference of the likelihoods of 500 realizations of the same model, differed by the Poisson statistics only, gives a range of likelihood around the maximum likelihood that defines the confidence level.

Table 2 lists our searching parameter space and the finest grid size we used. The key parameters in our study are n_0, H_{z1}, f_2 and H_{z2} (see Eqs. (1)-(2)). The first two play a primary role on the variation of the likelihood value and the latter two play a secondary role. The other five parameters H_{r1}, H_{r2}, f_h, κ and p (see Eqs. (1)-(3)) are non-key parameters, which play a minor role and do not affect the likelihood value as much as the key parameters.

4. The Results and Discussion

Table 3 lists our best-fit results with the corresponding uncertainties. Fig. 1 shows contour plots of likelihood against different pairs of parameters. The contour changes dramatically along the key parameters n_0, H_{z1}, f_2 and H_{z2}, but relatively mild along other parameters H_{r1}, H_{r2}, f_h, p and κ. This indicates the importance of the key parameters in determining the best-fit result.

Degeneracies exist between some pairs of key parameters, such as (n_0, H_{z1}), (n_0, f_2), $(H_{z1}, f_2)\ldots$etc. Here degeneracy means that the likelihood value stays almost the same when the pairs of parameters change together in a particular way. Similar degeneracy between the local thick-to-thin disk ratio f_2 and the scale-height of the thick disk H_{z2} has been reported in Chen et al. (2001); Siegel et al. (2002); Jurić et al. (2008); Bilir et al. (2008). Consequently, it is possible that different combinations of parameters can be regarded as 'acceptable' fitting. For example, if we choose a higher local stellar density n_0, then we can pick a smaller H_{z1} such that the likelihood value is very close to the maximum likelihood value and assign it as the 'best-match' scale-height of the thin disk. Therefore, a thin light color diagonal strip shows on the n_0 against H_{z1} contour plot in Fig. 1. Besides, similar trends happen in other pairs of key parameters. When one parameter of the pair is higher, we can get a similar likelihood value by lowering the other parameter (see the corresponding two-parameter contour plots of key parameters in Fig. 1). This anti-correlation is not unexpected. The number of stars along the line of sight in the model increases when any one of the key parameters increases. Thus for a given observed number of stars, an increase in one key parameter can be compensated by a decrease in the other. Perhaps this is the reason that our best-fit scale-height of the thin disk, $H_{z1} = 360$ pc, is somewhat larger than the reported values, $H_{z1} = 285$ pc, in Lopez-Corredoira et al. (2002) study (they also use star count of 2MASS to obtain

Galactic model parameters). Our best-fit local stellar density from K_s =-8 to 6.5 mag is $n_0 \sim 0.030$ star/pc^3, which is about half of ~ 0.056 star/pc^3 of the corresponding value cited in Eaton et al. (1984), and a bit lower than ~ 0.032 star/pc^3 of the corresponding value cited in Lopez-Corredoira et al. (2002). As a result, our fitting tends to choose a larger scale-height of the thin disk. If we force our local stellar density to be comparable with that of Lopez-Corredoira et al. (2002), then the corresponding 'best-fit' scale-height of the thin disk would be ∼320 pc, which is closer to their result. If we choose even higher local stellar density, then the 'best-fit' scale-height of the thin disk would be made between 200 to 300 pc, which is similar to the most of recent studies (see Table 1). Moreover, we do not apply binarism correction in our analysis, and it has been shown that scale-length and scale-height might be underestimated without binarism correction (Siegel et al. 2002; Jurić et al. 2008; Ivezić et al. 2008; Yaz & Karaali 2010).

For our purpose, we deem that in order to lift the degeneracy it is crucial to have a reliable near infrared luminosity function by observation or a near infrared local stellar density. Unfortunately, a systematic study in this direction is yet to come. Some related studies, such as synthetic luminosity function (see e.g., Girardi et al. 2005) or luminosity function transformed from optical observation (see e.g., Wainscoat et al. 1992) do exist, but some uncertainties still need to be settled (e.g., the initial mass function, mass-luminosity relation for NIR and color transformation between different wavelengths...etc.). Once the 'true' local stellar density is known, the 'true' structure of the Milky Way would be revealed.

In order to see how good the agreement between 2MASS data and our best-fit model, we show an all sky map of the ratios of observed to predicted integrated star count from K_s =5 to 14 mag for each node as a function of position on the sky in Fig. 2, and the color indicates the values of the ratios. We do not see obvious deviation in the Galactic latitude $|b| > 30^\circ$ areas, but only in the Large Magellanic Cloud and the Small Magellanic

Cloud areas. For comfirmation, we plot integrated star count from K_s =5 to 14 mag along Galactic longitude and latitude for $|b| > 30^\circ$ areas in Figs. 3 & 4. We see 2MASS data and our best-fit model agree well and only some small deviations in the nodes at the anti-Galactic center $b \sim 30^\circ$ areas. The significant spikes in Figs. 3 & 4 are due to the populations of the Large Magellanic Cloud and the Small Magellanic Cloud. For testing how these small deviations affect the key parameters selection, we exclude these small deviations and re-analyze the data with fixed non-key parameters. It shows only the scale-height of thick disk shifts slightly but still within our error estimation. Besides, we do not see any significant differences of reported overdensities in sky regions with $|b| > 30^\circ$. Thus, we conclude that the three-component model can describe the Milky Way structure sufficiently well for high Galactic latitude regions and the single power law luminosity function of Chang et al. (2010) is a good approximation as well. Since our main purpose is to search for the global Galactic model parameters, we do not try to explore the best-fit result for each node individually as what Cabrera-Lavers et al. (2007); Bilir et al. (2008); Yaz & Karaali (2010) have done in their studies to seek the variations of disk model parameters with Galactic longitude. Instead, we treat the differences of 2MASS data to our best-fit model as deviations from a global smooth distribution. We believe that similar variations in disk model parameters will be obtained if we take similar analysis procedure (i.e., searching best-fit parameters for each node), but this is beyond the scope of this work. Because we do not consider flares, warps and other overdensities in our model, there are some discrepancies between 2MASS data and the model in the low Galactic latitude regions (see Fig. 2). These fine structures make the star distribution more fluffy in the vertical direction toward the edge of the Milky Way. Hence the discrepancy between 2MASS data and the model increases vertically towards the anti-Galactic center region. In addition, the absence of Galactic bulge in our model contributes to the large discrepancy in Galactic center areas. The difference in the low Galactic latitude region needs more delicate analysis

to rectify (see, e.g., Lopez-Corredoira et al. 2002; Momany et al. 2006).

4.1. Summary

In summary, we set forth to study the global smooth structure of the Milky Way by a three-component stellar distribution model which comprises two double exponential disks (one thin and one thick) and an oblate halo. The K_s band 2MASS star count is used to determine the structure parameters. To avoid the complication introduced by the fine structures and complex extinction correction close to Galactic plane, we use only Galactic latitude $|b| > 30^\circ$ data. There are 10 parameters in the model, but only four of them play the dominant role in the fitting process. They are the local stellar density of the thin disk n_0, the local density ratio of thick-to-thin disk f_2, and the scale-height of the thin and thick disks H_{z1} and H_{z2}. The best-fit result is listed in Table 3. In short the scale-height of the thin and thick disks are 360 ± 10 pc and 1020 ± 30 pc, respectively; the scale-length of the thin disk is 3.7 ± 1.0 kpc and that of thick disk is 5.0 ± 1.0 kpc (the uncertainty in scale-length is large because it is not very sensitive to high latitude data.) The local stellar density ratio of thick-to-thin disk and halo-to-thin disk are $7 \pm 1\%$ and $0.20 \pm 0.10\%$, respectively. The local stellar density of the thin disk is 0.030 ± 0.002 stars/pc^3.

An all sky comparison of the 2MASS data to our best-fit model is shown in Fig. 2. A good agreement in the Galactic latitude $|b| > 30^\circ$ areas is expected from our fitting procedure. In low Galactic latitude regions, fine structures (such as flares, warps... etc.) increase the effective scale-height towards the edge of the Milky way. This is reflected in the fan-like increase in discrepancy towards the anti-Galactic center regions.

Degeneracy (i.e., different combinations of parameters give similar likelihood values) is found in pairs of key parameters (see Fig. 1). Thus different combinations of parameters

may fit the data almost as good as the best-fit one, and these are all legitimate 'acceptable' fitting in view of the uncertainty. Therefore, accompanying our lower local stellar density 0.030 stars/pc^3 (from $K_s = -8$ to 6.5 mag) is a higher thin disk scale-height 360 pc. In the context of NIR star count, the NIR luminosity function or the NIR local stellar density is imperative to determine the scale-height and other Milky Way structure parameters. We hope that systematic study on the luminosity function and the local stellar density in near infrared will be available in the near future.

We acknowledge the use of the Two Micron All Sky Survey Point Source Catalog (2MASS PSC). We would like to thank the anonymous referee, whose advice greatly improves the paper. CMK is grateful to S. Kwok and K.S. Cheng for their hospitality during his stay at the Department of Physics, Faculty of Science, University of Hong Kong. This work is supported in part by the National Science Council of Taiwan under the grants NSC-98-2923-M-008-001-MY3 and NSC-99-2112-M-008-015-MY3.

Table 1. Previous Galactic models. The parentheses are the corrected values for binarism. The asterisk denotes the power-law index replacing Re. References indicating with the original result table mean Galactic longitude or limiting magnitude dependent Galactic model parameters.

H_{z1} (pc)	H_{r1} (kpc)	f_2 (%)	H_{z2} (kpc)	H_{r2} (kpc)	f_h(%)	Re(S) (kpc)	κ	Reference
310 - 325	-	0.0125-0.025	1.92 - 2.39	-	-	-	-	Yoshii (1982)
300	-	0.02	1.45	-	-	-	-	Gilmore & Reid (1983)
325	-	0.02	1.3	-	0.002	3	0.85	Gilmore (1984)
280	-	0.0028	1.9	-	0.0012	-	-	Tritton & Morton (1984)
125-475	-	0.016	1.18 - 2.21	-	0.0013	3.1*	0.8	Robin & Creze (1986)
300	-	0.02	1	-	0.001	-	0.85	del Rio & Fenkart (1987)
285	-	0.015	1.3 - 1.5	-	0.002	2.36	Flat	Fenkart & Karaali (1987)
325	-	0.0224	0.95	-	0.001	2.9	0.9	Yoshii et al. (1987)
249	-	0.041	1	-	0.002	3	0.85	Kuijken & Gilmore (1989)
350	3.8	0.019	0.9	3.8	0.0011	2.7	0.84	Yamagata & Yoshii (1992)
290	-	-	0.86	-	-	4	-	von Hippel & Bothun (1993)
325	-	0.020-0.025	1.6-1.4	-	0.0015	2.67	0.8	Reid & Majewski (1993)
325	3.2	0.019	0.98	4.3	0.0024	3.3	0.48	Larsen (1996)
250-270	2.5	0.056	0.76	2.8	0.0015	2.44 - 2.75*	0.60 - 0.85	Robin et al. (1996, 2000)
260	2.3	0.074	0.76	3	-	-	-	Ojha et al. (1996)
290	4	0.059	0.91	3	0.0005	2.69	0.84	Buser et al. (1998, 1999)
240	-	0.061	0.79	-	-	-	-	Ojha et al. (1999)
280/267	-	0.02	1.26/1.29	-	-	2.99*	0.63	Phleps et al. (2000)
330	2.25	0.065 - 0.13	0.58 - 0.75	3.5	0.0013	-	0.55	Chen et al. (2001)
-	2.8	3.5	0.86	3.7	-	-	-	Ojha (2001)
280(350)	2 - 2.5	0.06 - 0.10	0.7 - 1.0 (0.9 - 1.2)	3 - 4	0.0015	-	0.50 - 0.70	Siegel et al. (2002)
285	1.97	-	-	-	-	-	-	Lopez-Corredoira et al. (2002)
-	3.5	0.02-0.03	0.9	4.7	0.002-0.003	4.3	0.5-0.6	Larsen & Humphreys (2003)
320	-	0.07	0.64	-	0.00125	-	0.6	Du et al. (2003)
265-495	-	0.052-0.098	0.805-0.970	-	0.0002-0.0015	-	0.6-0.8	Karaali et al. (2004, Table 16)
268	2.1	0.11	1.06	3.04	-	-	-	Cabrera-Lavers et al. (2005)
300	-	0.04-0.10	0.9	-	-	3/2.5*	1/0.6	Phleps et al. (2005)
220	1.9	-	-	-	-	-	-	Bilir et al. (2006a)
160-360	-	0.033-0.076	0.84-0.87	-	0.0004-0.0006	-	0.06-0.08	Bilir et al. (2006b, Table 15)
301/259	-	0.087/0.055	0.58/0.93	-	0.001	-	0.74	Bilir et al. (2006c, Table 5)
220-320	-	0.01-0.07	0.6-1.1	-	0.00125	-	>0.4	Du et al. (2006)
206/198	-	0.16/0.10	0.49/0.58	-	-	-	0.45	Ak et al. (2007)
140-269	-	0.062-0.145	0.80-1.16	-	-	-	-	Cabrera-Lavers et al. (2007, Table 1)
220-360	1.65-2.52	0.027-0.099	0.62-1.03	2.3-4.0	0.0001-0.0022	-	0.25-0.85	Karaali et al. (2007, Table 3)
167-200	-	0.055-0.151	0.55-0.72	-	0.0007-0.0019	-	0.53-0.76	Bilir et al. (2008, Table 1)
245(300)	2.15(2.6)	0.13(0.12)	0.743(0.900)	3.261(3.600)	0.0051	2.77*	0.64	Jurić et al. (2008)
325-369	1.00-1.68	0.0640-0.0659	0.860-0.952	2.65-5.49	0.0033-0.0039	-	0.0489-0.0654	Yaz & Karaali (2010, Table 1)
360	3.7	0.07	1.02	5	0.002	2.6*	0.55	This Work

Table 2. The searching parameter space.

	Range	Grid size
Thin Disk		
H_{r1}	1.0-6.0 kpc	100 pc
H_{z1}	200-450 pc	10 pc
n_0	0.02-0.04 stars/pc^3	0.002 stars/pc^3
$Z_\odot$	11-35 pc	2.5 pc
Thick Disk		
H_{r2}	3.0-7.0 kpc	200 pc
H_{z2}	400-1200 pc	20 pc
f_2	0-20%	1%
Spheroid		
κ	0.1-1.0	0.05
p	2.3-3.3	0.1
f_h	0-0.45%	0.05%

Table 3. The best-fit Milky Way model.

	Value	Uncertainty
Thin Disk		
H_{r1}	3.7 kpc	1.0 kpc
H_{z1}	360 pc	10 pc
n_0	0.030 stars/pc^3	0.002 stars/pc^3
$Z_\odot$	25 pc	5 pc
Thick Disk		
H_{r2}	5.0 kpc	1.0 kpc
H_{z2}	1020 pc	30 pc
f_2	7%	1 %
Spheroid		
κ	0.55	0.15
p	2.6	0.6
f_h	0.20%	0.10%

REFERENCES

Ak, S., Bilir, S., Karaali, S., & Buser, R. 2007, AN, 328, 169

Alves, D.R. 2000, ApJ, 539, 732

Bahcall, J.N., & Soneira, R.M. 1980, ApJ, 238, 17

Bienayme, O., Robin, A.C., & Creze, M. 1987, A&A, 180, 94

Bilir, S., Karaali, S., Ak, S., Yaz, E., & Hamzaoğlu, E. 2006, New A, 12, 234 (2006a)

Bilir, S., Karaali, S., & Gilmore, G. 2006, MNRAS, 366, 1295 (2006b)

Bilir, S., Karaali, S., Güver, T., Karataş, Y., & Ak, S. G. 2006, AN, 327, 72 (2006c)

Bilir, S., Cabrera-Lavers, A., Karaali, S., Ak, S., Yaz, E., & López-Corredoira, M. 2008, PASA, 25, 69

Buser, R., Rong, J., & Karaali, S. 1998, A&A, 331, 934

Buser, R., Rong, J., & Karaali, S. 1999, A&A, 348, 98

Cabrera-Lavers, A., Garzón, F., & Hammersley, P. L. 2005, A&A, 433, 173

Cabrera-Lavers, A., Bilir, S., Ak, S., Yaz, E., & López-Corredoira, M. 2007, A&A, 464, 565

Cabrera-Lavers, A., González-Fernández, C., Garzón, F., Hammersley, P. L., & López-Corredoira, M. 2008, A&A, 491, 781

Chang, C.-K., Ko, C.-M., & Peng, T.-H. 2010, ApJ, 724, 182

Chen, B., Figueras, F., Torra, J., Jordi, C., Luri, X., & Galadi-Enriquez, D. 1999, A&A, 352, 459

Chen, B., et al. (the SDSS collaboration) 2001, ApJ, 553, 184

Cutri, R.M., et al. 2003, The IRSA 2MASS All-Sky Point Source Catalog, NASA/IPAC Infrared Science Archive. http://irsa.ipac.caltech.edu/applications/Gator/

del Rio, G., & Fenkart, R. 1987, A&AS, 68, 397

Du, C., et al. 2003, A&A, 407, 541

Du, C., Ma, J., Wu, Z., & Zhou, X. 2006, MNRAS, 372, 1304

Eaton, N., Adams, D.J., & Giles, A.B. 1984, MNRAS, 208, 241

Fenkart, R., & Karaali, S. 1987, A&AS, 69, 33

Gilmore, G. 1984, MNRAS, 207, 223

Gilmore, G., & Reid, N. 1983, MNRAS, 202, 1025

Gilmore, G., & Wyse, R. F. G. 1985, AJ, 90, 2015

Girardi, L., Groenewegen, M.A.T., Hatziminaoglou, E., & da Costa, L. 2005, A&A, 436, 895

Hammersley, P.L., Garzón, F., Mahoney, T.J., López-Corredoira, M., & Torres, M.A.P. 2000, MNRAS, 317, L45

Herschel, W. 1785, Royal Society of London Philosophical Transactions Series I, 75, 213

Ivezić, Ž., et al. 2008, ApJ, 684, 287

Jurić, M., et al. 2008, ApJ, 673, 864

Kaiser, N., et al. 2002, Proc. SPIE, 4836, 154

Karaali, S., Bilir, S., & Hamzaoğlu, E. 2004, MNRAS, 355, 307

Karaali, S., Bilir, S., Yaz, E., Hamzaoğlu, E., & Buser, R. 2007, PASA, 24, 208

Kuijken, K., & Gilmore, G. 1989, MNRAS, 239, 605

Kunszt, P.Z., Szalay A.S., & Thakar A.R. 2001, Proc. of the MPA/ESO/MPE workshop (Springer-Verlag Berlin Heidelberg), pp. 631

Larsen, J. A. 1996, Ph.D. Thesis,

Larsen, J. A., & Humphreys, R. M. 2003, AJ, 125, 1958

Lopez-Corredoira, M., Cabrera-Lavers, A., Garzon, F., & Hammersley, P.L. 2002, A&A, 394, 883

Majewski, S. R., Skrutskie, M. F., Weinberg, M. D., & Ostheimer, J. C. 2003, ApJ, 599, 1082

Majewski, S. R., Ostheimer, J. C., Rocha-Pinto, H. J., Patterson, R. J., Guhathakurta, P., & Reitzel, D. 2004, ApJ, 615, 738

Martin, N. F., Ibata, R. A., Bellazzini, M., Irwin, M. J., Lewis, G. F., & Dehnen, W. 2004, MNRAS, 348, 12

Momany, Y., Zaggia, S., Gilmore, G., Piotto, G., Carraro, G., Bedin, L.R., & de Angeli, F. 2006, A&A, 451, 515

Newberg, H. J., et al. 2002, ApJ, 569, 245

Nishiyama, S., et al. 2005, ApJ, 621, L105

Ojha, D. K., Bienayme, O., Robin, A. C., Creze, M., & Mohan, V. 1996, A&A, 311, 456

Ojha, D. K., Bienaymé, O., Mohan, V., & Robin, A. C. 1999, A&A, 351, 945

Ojha, D.K. 2001, MNRAS, 322, 426

Phleps, S., Meisenheimer, K., Fuchs, B., & Wolf, C. 2000, A&A, 356, 108

Phleps, S., Drepper, S., Meisenheimer, K., & Fuchs, B. 2005, A&A, 443, 929

Perryman, M. A. C., et al. 2001, A&A, 369, 339

Reid, M. J. 1993, ARA&A, 31, 345

Reid, N., & Majewski, S. R. 1993, ApJ, 409, 635

Reylé, C., Marshall, D.J., Robin, A.C., & Schultheis, M. 2009, A&A, 495, 819

Robin, A., & Creze, M. 1986, A&A, 157, 71

Robin, A. C., Haywood, M., Creze, M., Ojha, D. K., & Bienayme, O. 1996, A&A, 305, 125

Robin, A. C., Reylé, C., & Crézé, M. 2000, A&A, 359, 103

Robin, A. C., Reylé, C., Derrière, S., & Picaud, S. 2003, A&A, 409, 523

Rocha-Pinto, H. J., Majewski, S. R., Skrutskie, M. F., & Crane, J. D. 2003, ApJ, 594, L115

Rocha-Pinto, H. J., Majewski, S. R., Skrutskie, M. F., Crane, J. D., & Patterson, R. J. 2004, ApJ, 615, 732

Schlegel, D.J., Finkbeiner, D.P., & Davis, M. 1998, ApJ, 500, 525

Siegel, M. H., Majewski, S. R., Reid, I. N., & Thompson, I. B. 2002, ApJ, 578, 151

Skrutskie M.F., et al. 2006, AJ, 131, 1163

Tritton, K. P., & Morton, D. C. 1984, MNRAS, 209, 429

van Loon, J. T., et al. 2003, MNRAS, 338, 857

von Hippel, T., & Bothun, G. D. 1993, ApJ, 407, 115

Yamagata, T., & Yoshii, Y. 1992, AJ, 103, 117

Yaz, E., & Karaali, S. 2010, New A, 15, 234

York, D. G., et al. 2000, AJ, 120, 1579

Yoshii, Y. 1982, PASJ, 34, 365

Yoshii, Y., Ishida, K., & Stobie, R. S. 1987, AJ, 93, 323

Wainscoat, R. J., Cohen, M., Volk, K., Walker, H. J., & Schwartz, D. E. 1992, ApJS, 83, 111

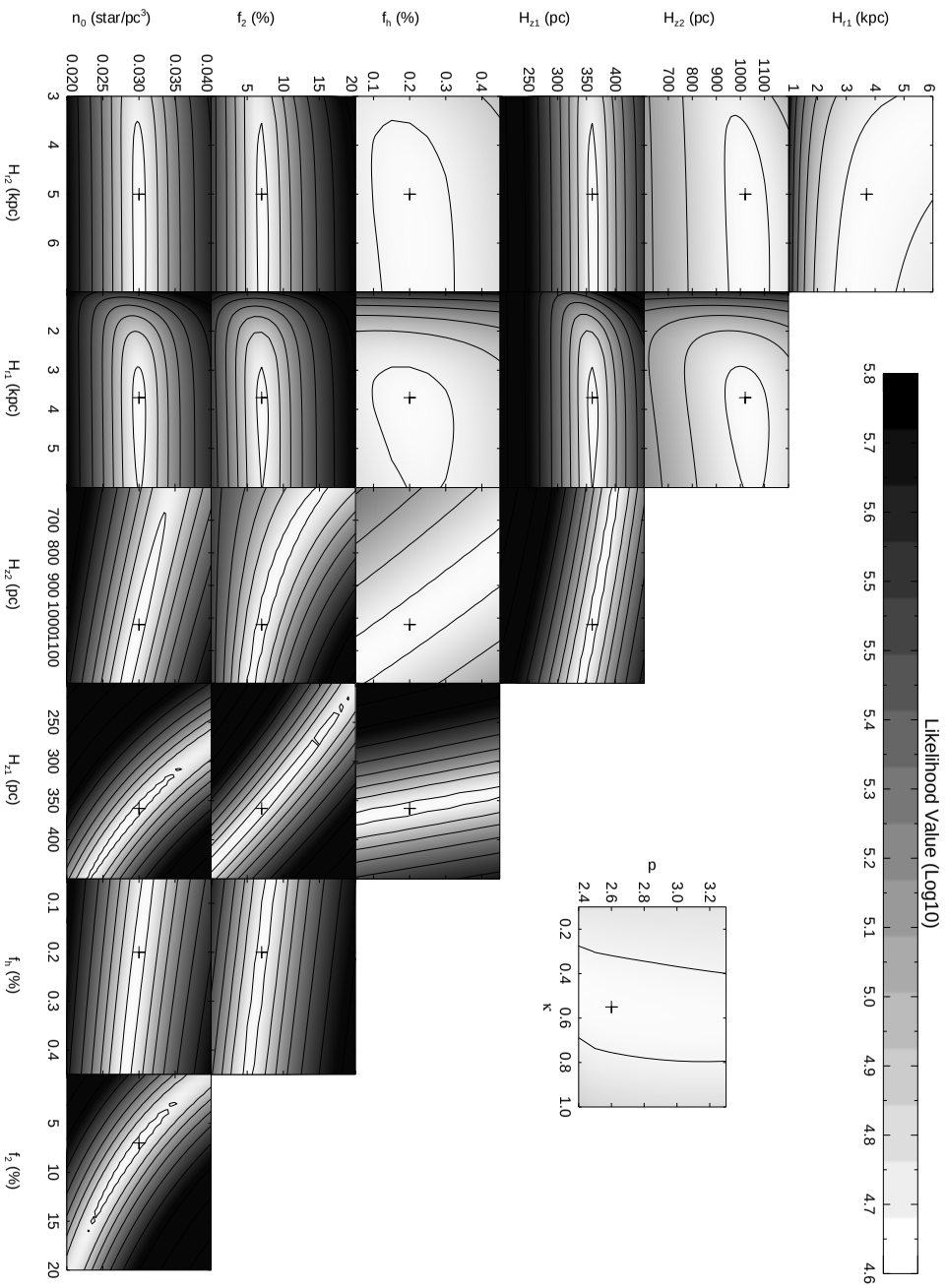

Fig. 1.— Contour plots of likelihood value of pairs of parameters in the Milky Way model. n_0, f_2, H_{z1}, H_{z2} are key parameters of the model. In this plot $R_\odot = 8$ kpc and $Z_\odot = 25$ pc. The cross marks our best-fit values. The innermost contour is at logarithmically maximum likelihood value 4.67, and the rest are logarithmically spaced in steps of 0.2 dex.

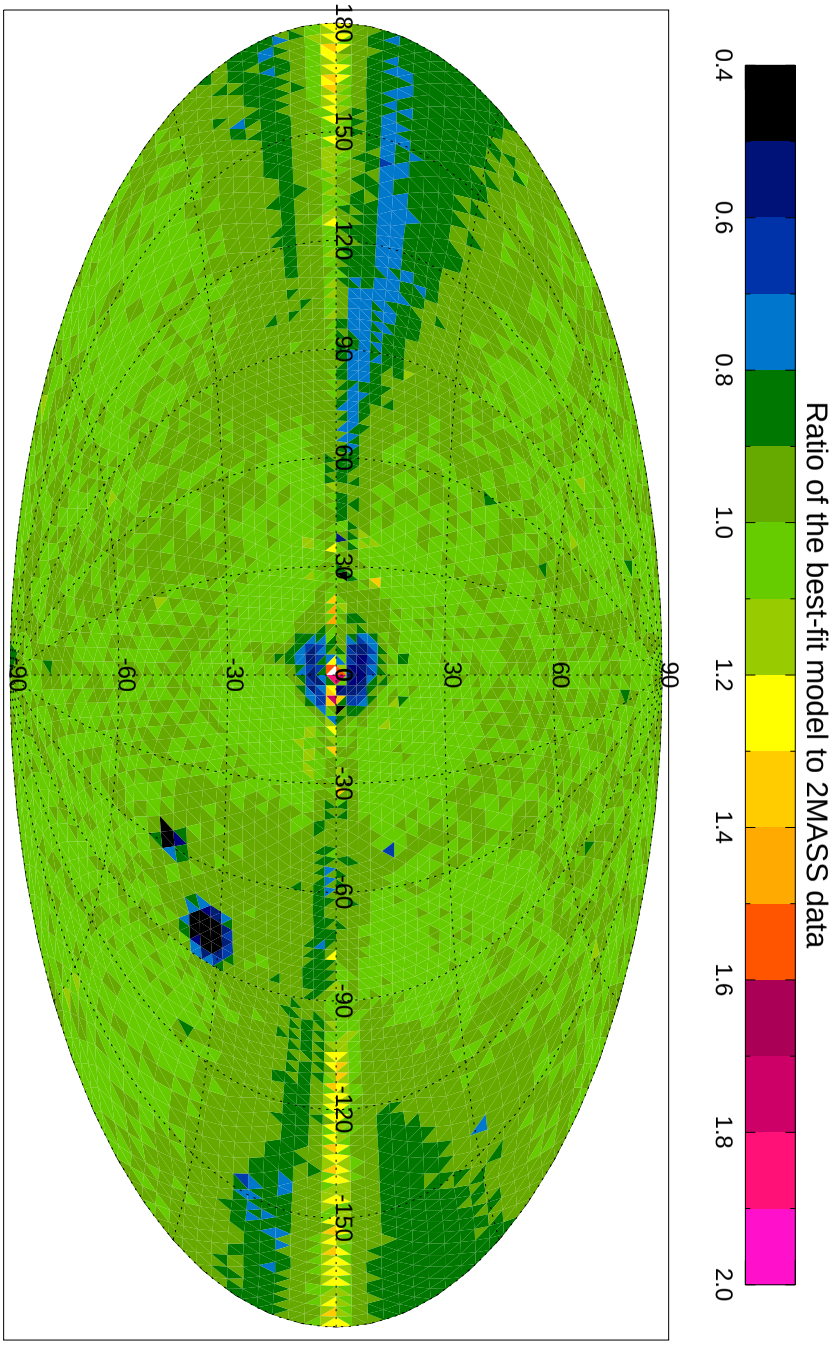

Fig. 2.— The ratios of observed to model integrated star count from K_s =5 to 14 mag.

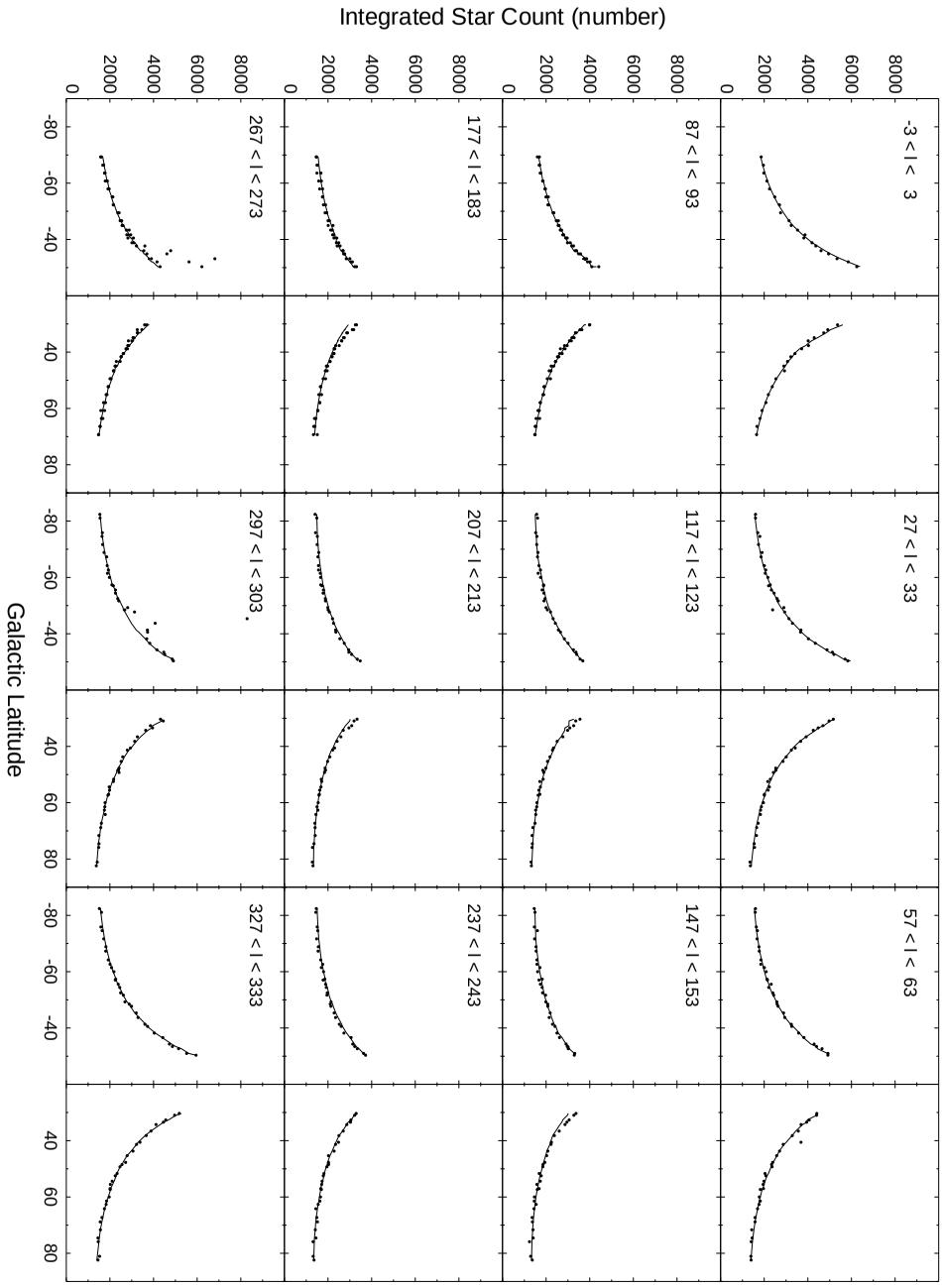

Fig. 3.— Integrated star count from K_s =5 to 14 mag of 2MASS data as a function of the Galactic latitude. Solid line is the model prediction.

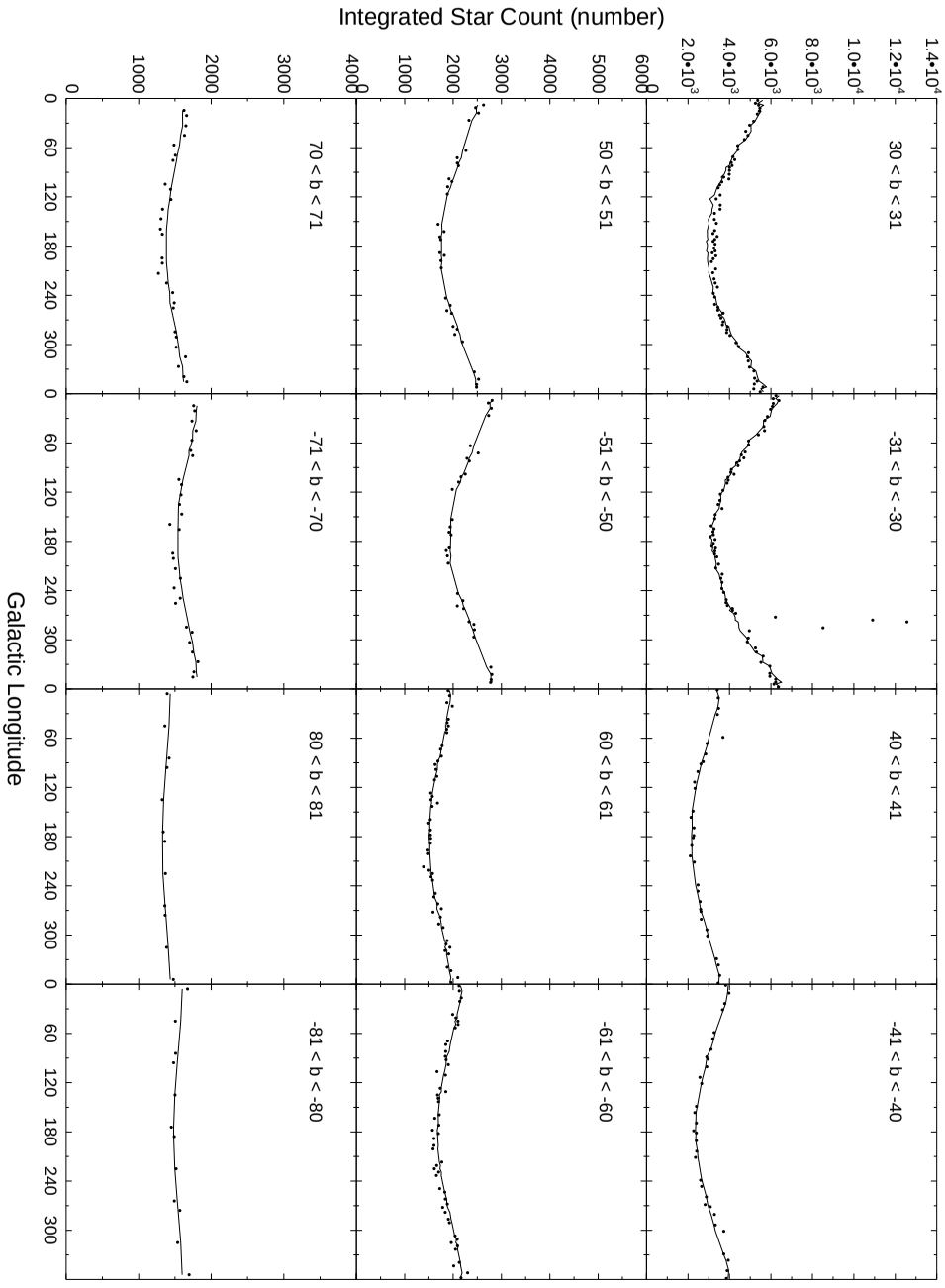

Fig. 4.— Integrated star count from K_s =5 to 14 mag of 2MASS data as a function of the Galactic longitude. Solid line is the model prediction.